International Journal of Pharmaceutics 422 (2012) 245–253

Contents lists available at SciVerse ScienceDirect

International Journal of Pharmaceutics

journal homepage: www.elsevier.com/locate/ijpharm

# The solid-state characterization of fusidic acid

Samuel E. Gilchrist, Kevin Letchford, Helen M. Burt*

*Faculty of Pharmaceutical Science, University of British Columbia, Vancouver, British Columbia, V6T 1Z3, Canada*

ARTICLE INFO

*Article history:*
Received 16 September 2011
Received in revised form 19 October 2011
Accepted 3 November 2011
Available online 10 November 2011

*Keywords:*
Fusidic acid
Polymorphism
Solid-state characterization
X-ray powder diffraction
Intrinsic dissolution

ABSTRACT

*Purpose:* The aim of this work was to characterize the solid-state properties of fusidic acid (FA).
*Methods:* Solid forms of FA were prepared by solvent-mediated polymorphic transformation of commercial FA (Form III) in acetonitrile (ACN), and methanol:$H_2O$ (50:50), or generated by solvent recrystallization from dichloromethane (DCM). Polymorphs were characterized using, X-ray diffraction (XRD), differential scanning calorimetry (DSC), thermal gravimetric analysis (TGA), polarizing hot stage microscopy (HSM), and intrinsic dissolution rate (IDR).
*Results:* Slurrying commercial FA (Form III) in methanol:$H_2O$ (50:50), yielded a metastable form (Form IV). This metastable form converts to Form I or back to Form III in ACN and $H_2O$, respectively, and Form II upon recrystallization from DCM. IDR of Form IV was 0.092 mg/min/cm$^2$, and was statistically different ($p < 0.05$) from the IDR of Forms I, II, and III, with IDR of 0.053, 0.043, and 0.045 mg/min/cm$^2$, respectively. The amorphous FA had an IDR of 0.125 mg/min/cm$^2$, and was significantly higher ($p < 0.05$) than any other solid form. There were no statistical differences in the IDR of Form I, II, or III.
*Conclusions:* This work provides evidence for the existence of two previously unreported polymorphic forms of FA (Forms II and IV) and an amorphate.



## 1. Introduction

With the increased average age of the population, the number of total joint arthroplasties has steadily increased over the past few decades as the population ages. However, a disproportionate increase in surgical site infections (SSI) has prevented the success of numerous restoration procedures. Between 1990 and 2004, the incidence of SSI following revision total knee and total hip arthroplasty increased 300% and 700% respectively, despite only a doubling in the number of surgical procedures (Kurtz et al., 2008). The persistence of SSI following invasive surgery is due, at least in part, to the emergence of multi-drug resistant microorganisms. For instance, in *Staphylococcus aureus* alone, there are reports of resistance to β-lactams (Ayliffe, 1997), macrolides (Schmitz et al., 2000), vancomycin (Khatib et al., 2011), daptomycin (Yang et al., 2010), and linezolid (Toh et al., 2007). In addition, clinical isolates from orthopaedic sites have shown that methicillin-resistant *S. aureus* (MRSA) is present in >24% of infections, and >70% of those MRSA isolates display multi-drug resistance (Sisirak et al., 2010). Therefore, there is a clinical need for alternative treatment strategies. Currently, there is much interest in the use of old generation antibiotics in surgical prophylaxis and treatment due to the decreased incidence of antibiotic resistance to these drugs (Maviglia et al., 2009). One class of antibiotics that has garnered attention is the steroidal antibiotics, specifically fusidic acid (FA). FA is a tetracyclic triterpenoid derived from the fermentation broth of the fungus *Fusidium coccineum*. It has been available since the 1960's as either the sodium salt or free acid and is commercially available in Canada, Australia, and the UK as oral, topical, ophthalmic and intravenous dosage forms, and is most often prescribed for skin and eye infections (Spelman, 1999). However, it has yet to be approved for use in the United States (Howden and Grayson, 2006). FA has high antimicrobial activity against Gram-positive bacteria, in particular *S. aureus*, *Staphylococcus epidermidis*, and coagulase-negative *staphylococci* including strains that are methicillin-resistant (Coombs, 1990), and strains that display multi-drug resistance (Sisirak et al., 2010). It is due to this spectrum of activity that FA has become increasingly popular in the treatment of bone and prosthetic joint infections as Gram-positive organisms are commonly the culprits of orthopaedic infections.

Current guidelines state that FA is indicated for the treatment of prosthetic joints infections when MRSA is the infecting microorganism, and is dosed orally at 500 mg every 8 h for a minimum of 3 months (Zimmerli and Ochsner, 2003; Trampuz and Zimmerli, 2006; Mastrokalos et al., 2006). However, despite this

*Abbreviations:* FA, fusidic acid; XRD, single-crystal X-ray diffraction; XRPD, X-ray powder diffraction; SEM, scanning electron microscopy; TGA, thermogravimetric analysis; DSC, differential scanning calorimetry; HSM, hot-stage microscopy; IDR, intrinsic dissolution rate; $T_g$, glass transition temperature; $\Delta H_f$, enthalpy of fusion; $\Delta H_r$, enthalpy of recrystallization.

* Corresponding author. Tel.: +1 604 822 2440; fax: +1 604 822 3034.
*E-mail address:* burt@interchange.ubc.ca (H.M. Burt).

0378-5173/$ – see front matter © 2011 Elsevier B.V. All rights reserved.
doi:10.1016/j.ijpharm.2011.11.005

dose being equivalent to intravenous dosing, maintaining minimum inhibitory concentrations at the site of infection as well as systemic side effects are often of concern. Therefore, a primary focus of our lab is the development of a locally applied drug delivery system of FA for the treatment of orthopaedic infections. The local administration of antibiotics to the site of infection is an attractive option for the treatment of bone infections due to the ability to maintain high tissue levels for prolonged periods of time, while simultaneously avoiding systemic side effects. To date, several locally applied antibiotic delivery systems have been investigated including ciprofloxacin, gentamicin and vancomycin loaded poly(methylmethacrylate) bone cement beads (Mader et al., 1997), gentamicin loaded collagen sponges (Mendel et al., 2005), vancomycin and tobramycin loaded allograft bone (Winkler et al., 2008), and ciprofloxacin loaded poly(lactic acid) pellets (Koort et al., 2005). In many cases, these systems consist of solid drug particles dispersed throughout the device matrix, such as in the case of ciprofloxacin and fosfomycin loaded polyurethane films (Schierholz et al., 1997), cefazolin and ciprofloxacin loaded glycerol monosterate implants (Allababidi and Shah, 1998), and gentamicin loaded poly(L-lactic acid) films (Aviv et al., 2007). Recently, our group has demonstrated that when FA is formulated in poly(lactic acid-co-glycolic acid) microspheres and films cast from dichloromethane (DCM), the drug phase separates into drug-rich microdomains, suggesting that FA is present in the solid-state within the polymer (Yang et al., 2009).

Even though FA has been in use for several decades and there is renewed interest in its use in post-surgical infections, its solid-state properties have not been reported in the peer-reviewed literature. FA is commercially available as a crystalline free acid ($C_{31}H_{48}O_6$), with a molecular weight of 516.72 Da (anhydrous) and a p$K_a$ of 5.35 (O'Neil, 2006). The patent literature (Jensen and Andersen, 2006) and one monograph (Reeves, 1987) claim that FA free acid exists as a hemihydrate. In this work, we characterize the solid state properties of commercially available FA, and prepare and characterize 2 new polymorphs and the amorphous form of FA.

## 2. Materials and methods

### 2.1. Materials

Commercially available FA was kindly supplied by Ercros, Pharmaceuticals Division (Madrid, ES). The solvents acetone (ACE), acetonitrile (ACN) chloroform ($CHCl_3$), DCM, ethanol (EtOH), ethyl acetate (EA), hexane (HEX), methyl *tert*-butyl ether (MTBE), toluene (TOL), 1-propanol, 1-butanol and phosphoric acid were of HPLC grade and purchased from Fisher Scientific (Ottawa, ON).

### 2.2. Methods

#### 2.2.1. Generation of FA solid forms

*2.2.1.1. Solvent-mediated polymorphic transformation.* Commercially sourced FA was slurried in anhydrous ACN, or MeOH:$H_2O$ (50:50) at 50 mg/mL in 1 mL chromatography vials with plastic cap. The vials were tumbled end-over-end at room temperature and 10 rpm using a benchtop rotor (Labquake®; Barnstead Thermolyne). At predetermined time points, the suspension was filtered using a 0.45 μm white nylon filter (Millipore Corp.; Billerica, MA) and the solid was subsequently dried under 635 mmHg vacuum at room temperature in the presence of a desiccant until analysis (24 h minimum).

*2.2.1.2. Recrystallization of FA polymorphs via solvent evaporation.* Fusidic acid was recrystallized from the following solvents: ACE, ACN, $CHCl_3$, DCM, EtOH, EA, HEX, MTBE, TOL, 1-propanol, and 1-butanol. Recrystallization of FA was achieved by dissolving the drug in 2 mL of solvent in a 20 mL glass scintillation vial at a concentration of 50–100 mg/mL followed by evaporation of the solvent at either room temperature or −20 °C. Amorphous FA was prepared by dissolving 250 mg of FA in 1 mL of DCM in a 20 mL glass vial followed by rapid removal of the solvent at 100 °C in an oil bath under a stream of nitrogen. All recrystallized forms and the amorphous form of FA were stored under 635 mmHg vacuum at ambient temperature until analysis.

#### 2.2.2. Characterization of polymorphs

*2.2.2.1. Single crystal X-ray diffraction (XRD).* A FA crystal, obtained through the evaporation of solvent from a FA/ACN solution, was mounted on a glass fiber. Measurements were made on a Bruker APEX DUO diffractometer with cross-coupled multilayer optics Cu-Kα radiation. The data were collected at a temperature of $-183.0 \pm 0.1$ °C to a maximum $2\theta$ value of 132.0°. Data were collected in a series of $\phi$ and $w$ scans in 1° oscillations using 3.0 s exposures. The crystal-to-detector distance was set to 59.65 mm.

*2.2.2.2. X-ray powder diffraction (XRPD).* X-ray powder diffraction (XRPD) patterns of FA solid forms were obtained at 25 °C with a Bruker (Milton, ON) APEX DUO diffractometer with cross-coupled multilayer optics Cu-Kα radiation. Samples were packed into a thin-walled capillary tubes (special glass; Charles Supper Company, Natick, MA) and sealed using a small amount of capillary wax. Samples were scanned from 4° to 60° $2\theta$ using a step size of 0.02° and a step time of 3 s/step. Data were collected and analyzed with Bruker Diffrac Plus XRD Commander version 2.3 software.

*2.2.2.3. Scanning electron microscopy (SEM).* The crystal habits of FA polymorphs were evaluated using SEM. Samples were scattered onto a SEM stub and sputter-coated with a layer of 60:40 gold:palladium alloy using a Denton Vacuum Desk II sputter-coater (Moorestown, NJ) at 50 mTorr. SEM images were captured using a Hitachi S-3000N system (Tokyo, Japan) scanning at 5–20 keV.

*2.2.2.4. Thermal gravimetric analysis (TGA).* Samples were analyzed for weight loss during heating using a TA Instruments (New Castle, DE) Q50 thermal gravimetric analyzer. Approximately 5 mg of sample was weighed into an open pan and heated from 40 °C to 250 °C at 10 °C/min under nitrogen gas purge flowing at 20 mL/min.

*2.2.2.5. Differential scanning calorimetry (DSC).* Differential scanning calorimetry (DSC) thermograms of FA samples were recorded using a TA Instruments Q100 differential calorimeter with a refrigerated cooling system. Approximately 5 mg of sample was weighed into a hermetically sealed pan with a pinhole. Samples were equilibrated at 40 °C for 1 min followed by heating to 250 °C at a rate of 10 °C/min. The heat flow, and heat capacity of the instrument was calibrated using a high purity indium standard.

*2.2.2.6. Hot stage microscopy (HSM).* Thermal events were visually monitored by hot stage microscopy. Samples were placed on a glass microscope slide, equilibrated at 100 °C and then heated at 10 °C/min to 250 °C using a Metler Toledo (Columbus, OH) FP900 Thermosystem hot stage with temperature controller. Samples were viewed using an Olympus CX41 transmission light microscope with magnification of 10× and a polarizing filter over the light source. The thermal events were digitally recorded using Olympus Stream Basic imaging and documentation software (v. 1.6).

*2.2.2.7. Polymorphic stability in aqueous slurry.* FA as Forms I, III, IV, and amorphous solids were slurried in $H_2O$ at 50 mg/mL as

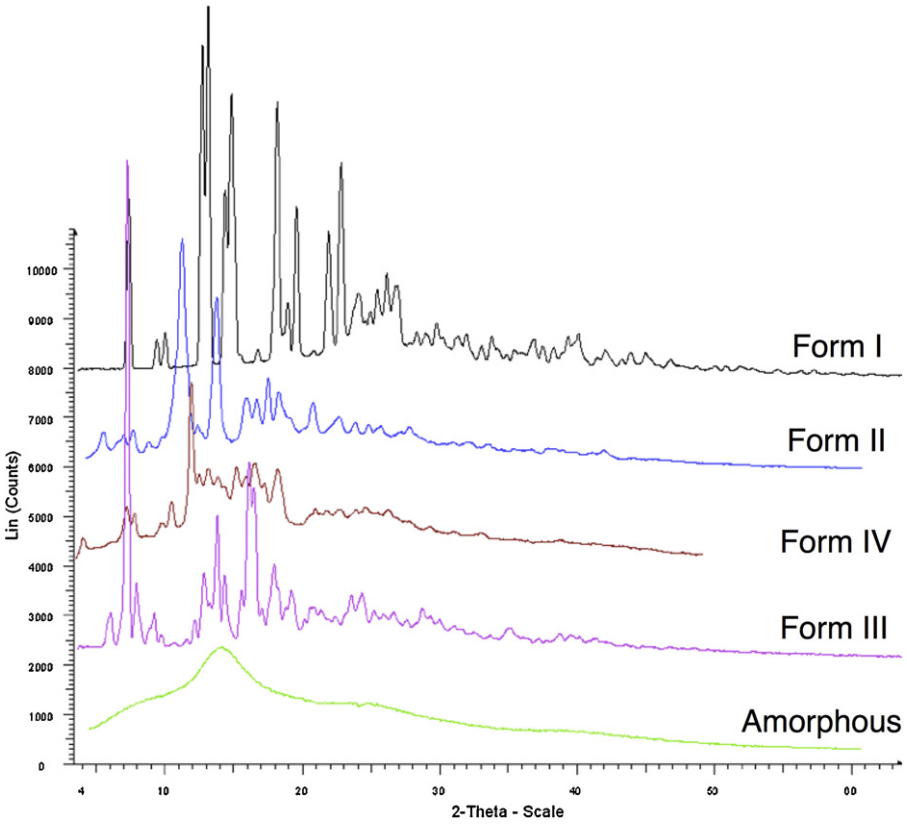


**Fig. 1.** XRPD patterns of FA, Forms I–IV and amorphous FA.

described above. At pre-determined time points, the FA suspensions were filtered, dried, and analyzed using XRPD as described above.

*2.2.2.8. Intrinsic dissolution rate (IDR).* Solid forms of FA were evaluated for intrinsic dissolution rate using a Wood's intrinsic dissolution apparatus (Hanson Research; Chatsworth, CA) and a Mandel SR8 Plus Dissolution Test Station (Guelph, ON). A 50 mg sample of FA was compressed at 1500 psi for 60 s in a 8 mm electropolished die using an Enerpac P142 hydraulic press (Butler, WI). The die housing the drug compact was attached to a shaft and holder and submerged in 500 mL degassed phosphate buffered saline (PBS; pH 7.4) at 37 °C with the rotation speed set to 50 rpm. At pre-determined time points, 2 mL of the dissolution media were withdrawn and analyzed for FA content using an HPLC (Waters® Millennium System) assay utilizing a mobile phase of 50/30/20 (v/v/v) ACN/MeOH/0.01 M phosphoric acid solution, flowing at 1 mL/min through a C18 reverse phase Vovapak column (Waters®), with a 20 μL sample injection volume and detection λ at 235 nm. FA was quantified against a standard curve prepared by dissolving FA in ACN over a range of 0.1–500 μg/mL. Data were analyzed using Waters Millennium 32 software.

### 2.3. Statistical analysis

IDR values were calculated by a linear regression analysis of the amount of FA dissolved (mg) per unit surface area of the compressed disk, over 30-min in the IDR experiments. Differences between the IDR of each of the FA polymorphs were evaluated using a one-way ANOVA and a Newman–Keuls multiple comparison *post-hoc* test with significance level set a $p < 0.05$. All analysis was done using GraphPad Prism v. 5 for Mac OS X (GraphPad Software, San Diego CA, USA).

## 3. Results

### 3.1. X-ray diffraction

#### 3.1.1. Powder XRD

XRPD patterns for the 4 solid samples were different, indicative of the presence of 4 different solid forms of FA. Based on single crystal XRD and thermal analysis findings, given below, we found no evidence of hydrate or solvate forms of FA. Hence the different XRPD patterns were indicative of 4 FA polymorphic forms, which have been designated Forms I–IV. The naming of these forms is based on their melting points as determined by DSC (see Section 3.3.2), with Form I having the highest melting point, and Form IV having the lowest. Major diffraction peaks were present at 7.23°, 12.67°, 13.12°, 18.18°, and 22.82° 2$\theta$ for Form I, 11.18°, 13.7°, 15.82°, 17.4°, and 18.19° 2$\theta$ for Form II, 7.18°, 13.7°, 15.99°, 16.42°, and 17.91° 2$\theta$ for Form III, and 11.78°, 13.1°, 15.12°, 16.44°, and 18.11° 2$\theta$ for Form IV (Fig. 1). Amorphous FA lacked any diffraction peaks and was characterized by a characteristic broad halo. A summary of XRPD data is shown in Table S1, which is available online in Supplementary Data.

Slurrying Form I or Form III in water for up to 28 days did not result in a change in the XRPD pattern (Fig. 2). However, the same treatment of either Form IV or amorphous FA resulted in a significant time dependent change in the diffraction pattern of these forms, with the appearance of peaks consistent with those of Form III. The identification of the various polymorphs with respect to their source, and crystallization conditions are summarized in Table 1.

#### 3.1.2. Single crystal XRD

Only FA recrystallized from ACN generated a single crystal large enough to perform single crystal XRD analysis. To investigate the

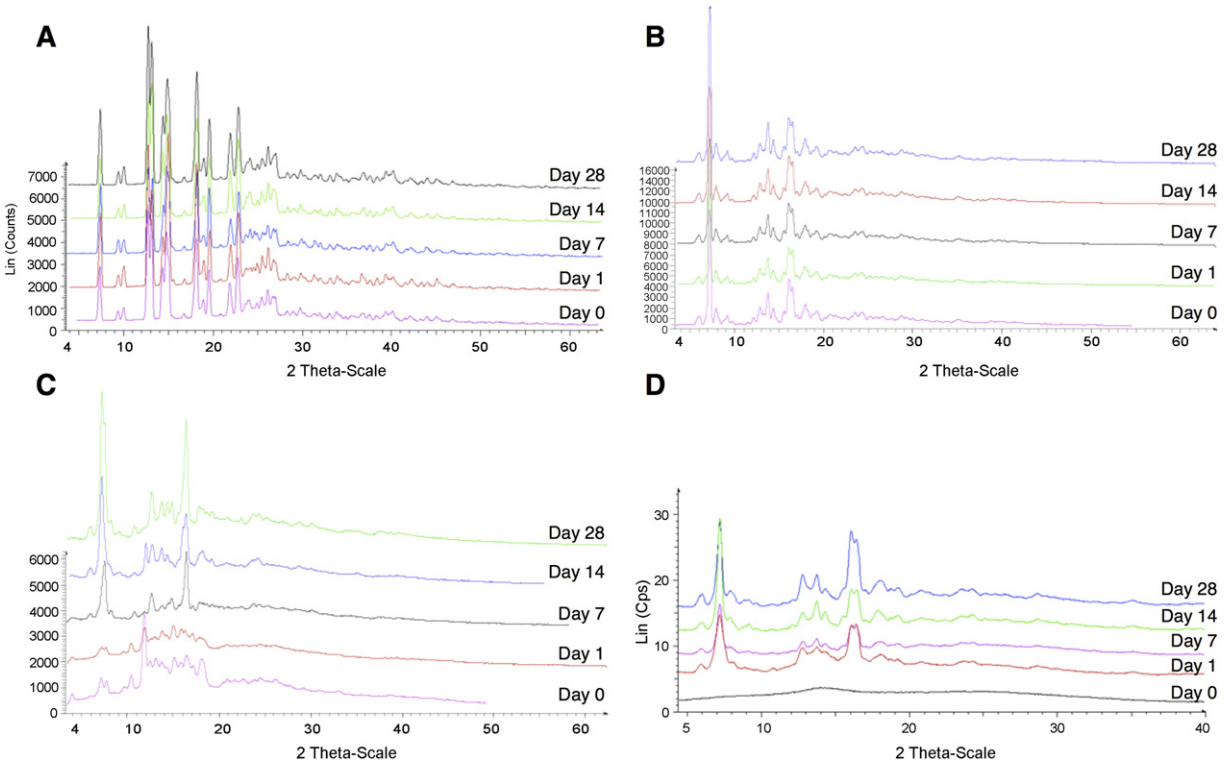


**Fig. 2.** XRPD patterns of (A) Form I, (B) Form III, (C) Form IV, and (D) amorphous FA, slurried in $H_2O$ for 1, 7, 14, and 28 days.

packing orientation of FA in this polymorph, a crystal with approximate dimensions of 0.12 mm × 0.18 mm × 0.46 mm was mounted on a glass fiber. Fig. 3 shows the crystal structure of FA, highlighting the oxygen atoms (O1–O6) involved in inter-molecular hydrogen bonding between FA molecules in the unit cell. The unit cell of Form I is a primitive monoclinic lattice system containing two FA molecules (Fig. 1B), with lattice parameters as follows: $a$ = 12.23 Å; $b$ = 8.0 Å; $c$ = 13.9 Å; $\alpha$ = 90°; $\beta$ = 94.3°; $\gamma$ = 90°; $V$ = 1357.7 Å$^3$.

### 3.2. Scanning electron microscopy

SEM micrographs of the solid forms of FA are shown in Fig. 4. Form I, produced by solution-mediated polymorphic transformation of Form III in ACN, produced needle- or rod-like crystals. Form II, formed by recrystallizing Form III from DCM was comprised of single- and multi-layered plates. Form III, either the commercially available form or through $H_2O$-mediated polymorphic transformation of Form IV or amorphous FA, was composed of very small plates, with some scattered irregular particles. Form IV, produced by solution-mediated polymorphic transformation of Form III in MeOH:$H_2O$ (50:50), yielded hexagonal plates. Amorphous FA was a mixture of particles, with no distinct crystal habit. The FA solid forms produced from the evaporation from all over solvents are not shown, as XRPD showed no crystalline characteristics.

### 3.3. Thermal analysis

#### 3.3.1. Thermal gravimetric analysis (TGA)

Upon heating, all FA polymorphs, except Form II, displayed a gradual weight loss between 40 °C and 150 °C of 0.7%, 2.5%, 1.6%, and 1.2%, for Forms IV, I, III, and the amorphous form, respectively. After this small initial weight loss, the mass remained constant until approximately 178 °C for Forms IV, II, III, and amorphous FA. Rapid mass loss did not occur until approximately 190 °C for Form I. Thermal degradation events observed by TGA are summarized in Table 1.

**Table 1**
Summary of thermal events for FA solid forms.

| Polymorph | Preparation | Transition[a] | Transition temperature (°C) | $\Delta H$ (J/g)[b] | Degradation temperature (°C)[c] |
|---|---|---|---|---|---|
| Form IV | Slurry Form III in MeOH/$H_2O$ | $T_{m,1}$ | 128.2 ± 0.2 | 11.0 ± 1.7 ($\Delta H_f$) | – |
| | | $T_c$ | 153.4 ± 1.0 | 40.0 ± 1.4 ($\Delta H_r$) | – |
| | | $T_{m,2}$ | 175.1 ± 0.3 | 42.7 ± 4.8 ($\Delta H_f$) | 178.4 ± 5.4 |
| Form I | Slurry any form in ACN | $T_m$ | 190.0 ± 0.1 | 50.3 ± 2.5 ($\Delta H_f$) | 188.9 ± 0.5 |
| Form II | Recrystallized any form from DCM at −20 °C | $T_m$ | 179.2 ± 0.6 | 58.5 ± 5.4 ($\Delta H_f$) | 179.9 ± 1.0 |
| Form III | As received from Ercros or slurry Form IV or amorphous in $H_2O$ | $T_m$ | 148.7 ± 1.2 | 18.9 ± 3.7 ($\Delta H_f$) | 174.5 ± 0.5 |
| Amorphous | Rapid evaporation of any form in DCM | $T_g$ | 116.9 ± 2.1 | – | 171.4 ± 0.7 |

Results are expressed as the mean ± S.D. $n$ = 3.

[a] $T_m$, melting temperature, the peak temperature of an exothermic transition; $T_r$, recrystallization temperature, the peak temperature of an exothermic transition; $T_g$, glass transition temperature, the midpoint of the transition as determined by differential scanning calorimetry (DSC).

[b] Where endothermic transitions were observed, enthalpy values represent the heat of fusion ($\Delta H_f$), whereas exothermic transitions are expressed as the heat of recrystallization ($\Delta H_r$).

[c] Onset temperature of mass loss as determined by thermogravimetric analysis (TGA).

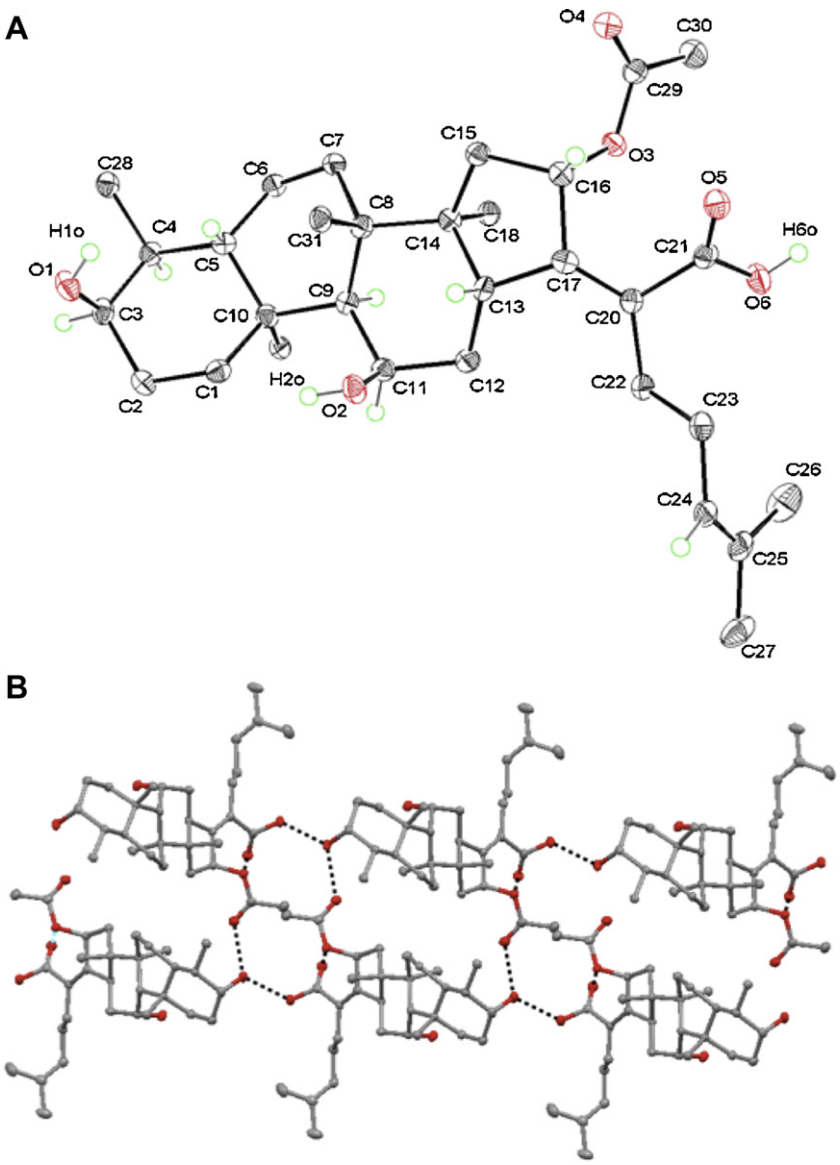


**Fig. 3.** (A) Single crystal structure of FA Form I; (B) packing diagram for FA Form I. View is looking down the B-axis and illustrates the orientation of fusidic acid molecules and hydrogen bonding between molecules in 3 consecutive unit cells.

### 3.3.2. *Differential scanning calorimetry (DSC)*

The thermal behavior of the FA polymorphs differed as demonstrated by the thermograms in Fig. 5. Forms I, II, and III were characterized by endothermic thermal events at 190 °C, 179 °C, and 148 °C, respectively. Form IV displayed three thermal events with an endothermic transition with a peak at 128 °C, an exotherm at 153 °C, followed by an endotherm at 175 °C. The thermogram of the amorphous FA showed a baseline shift, indicative of a glass transition temperature, at approximately 117 °C. All solid forms showed a broad endotherm around 193 °C, corresponding to significant weight loss and thermal degradation. The thermal events observed by DSC are summarized in Table 1.

### 3.4. *Hot stage microscopy (HSM)*

The thermal transitions of each of the solid-state forms of FA were observed using hot stage microscopy (Fig. 6). Polarized light was used to distinguish crystalline material, which appeared as bright birefringent areas, from non-crystalline material, which appeared as dark grey regions. Forms I and II remained birefringent throughout the heating cycle until the samples melted at 178 °C (Form II), or 190 °C (Form I). Form III initially showed only small areas of birefringence, but upon melting at 130 °C, the birefringent areas became more visible. Form IV melted at 130 °C. This thermal event was followed by recrystallization at 153 °C as indicated by the reappearance of birefringence, and a final melt at 178 °C. The amorphous form of FA was devoid of birefringence throughout the entire heating cycle.

### 3.5. *Intrinsic dissolution rate (IDR)*

IDR plots are shown in Fig. 7. The IDR of Form IV was found to be 0.092 mg/min/cm$^2$, and was statistically different ($p < 0.05$) from the IDR of Forms I, II, and III, which had IDR values of 0.053, 0.043, and 0.045 mg/min/cm$^2$, respectively (Fig. 7). The amorphous FA had an IDR of 0.125 mg/min/cm$^2$, and was significantly higher ($p < 0.05$) than any other solid form. There was no statistical difference in the IDR of Form I, II, or III.

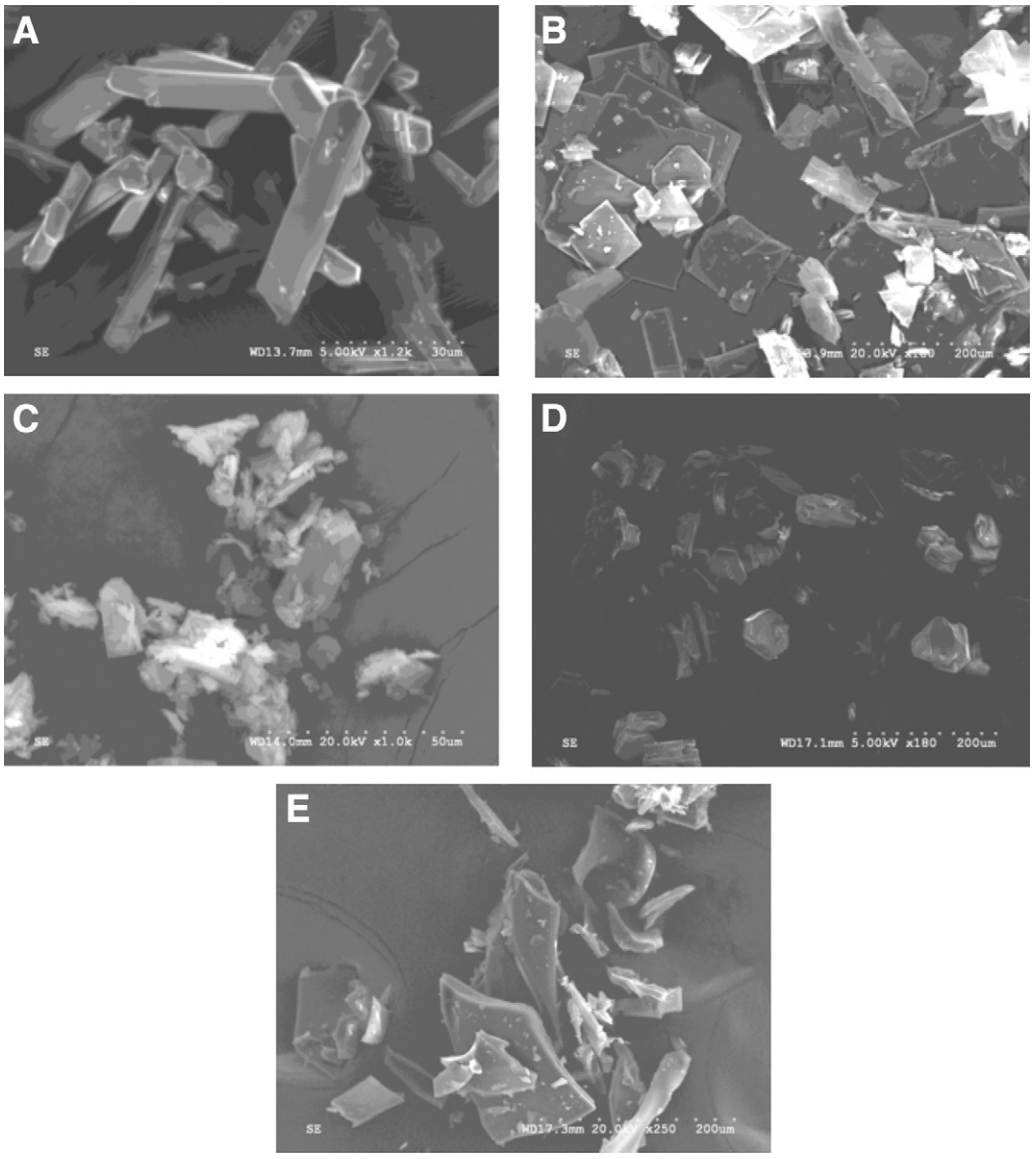


**Fig. 4.** Scanning electron micrographs showing the morphologies and crystal habits of (A) Form I, (B) Form II, (C) Form III, (D) Form IV, and (E) amorphous FA.

## 4. Discussion

The generation of FA solid forms was achieved through solvent-mediated polymorphic transformation (for solvents with low FA solubility; <50 mg/mL) or recrystallization from solvents (for solvents with high FA solubility; >50 mg/mL). In the latter case, we were restricted to DCM as recrystallization from other solvents (i.e. chloroform, ethyl acetate, ethanol, methanol, toluene, methyl *tert*-butyl ether, hexane, acetone, 1-propanol, and 1-butanol) yielded only amorphous solid forms, and were not evaluated further. The recrystallization of FA from DCM is a novel method for the production of crystalline FA, which has not been reported in literature. During solvent-mediated polymorphic transition, the solution is saturated with respect to the metastable polymorph, and supersaturated with respect to the most stable polymorphic form. Thus, with time, the most stable form will nucleate and precipitate out to maintain thermodynamic equilibrium (Miller et al., 2005). In order to perform these studies, we slurried commercial FA in $H_2O$, ACN, and MeOH:$H_2O$ (50:50). In ACN, Forms III, IV and amorphous FA, all generated Form I within 24 h (Fig. 8). However, using $H_2O$, only Form IV and amorphous forms of FA transformed to generate Form

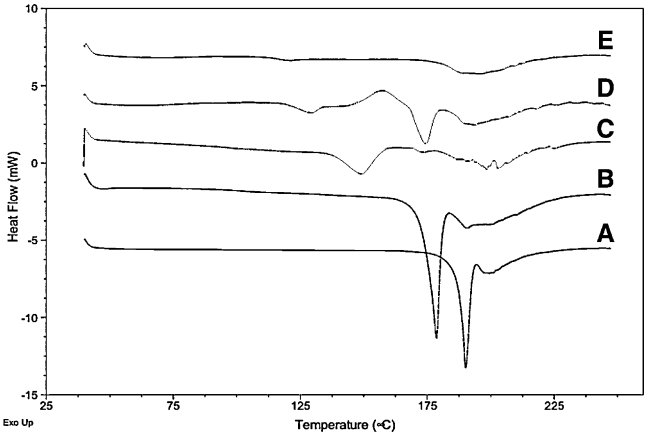


**Fig. 5.** DSC thermograms of (A) Form I, (B) Form II, (C) Form III, (D) Form IV, and (E) amorphous FA.

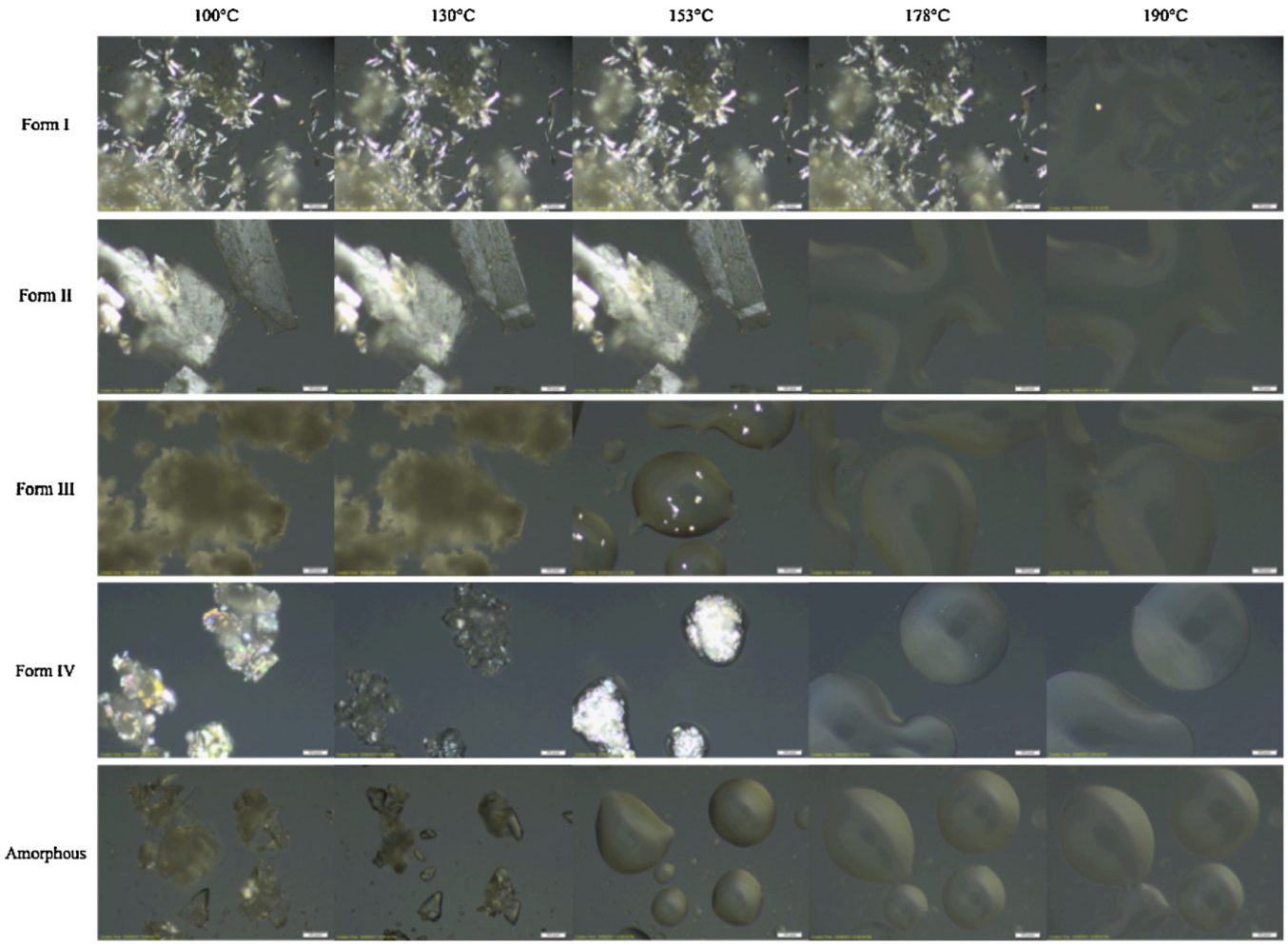


**Fig. 6.** Hot stage micrographs of the solid forms of FA at 100 °C, 130 °C, 153 °C, 178 °C and 190 °C. The scale bar (white rectangle) is 100px across, and represents 50 μm.

III over 28 days (Fig. 8), as determined by XRPD (Fig. 4). A number of peer-reviewed reports highlight the importance of proper solvent selection in screening for stable polymorphic forms (Gu et al., 2001; Miller et al., 2005). These authors suggest that the hydrogen-bonding propensity (HBP) of the solvent and the overall solubility of the drug are the critical determinants for producing the most stable polymorph. Solvents with high HBP but very poor drug solubility will retard polymorphic transformation favoring a metastable form. Conversely, solvents with weak HBP and higher solubility will favor a more stable polymorph (Gu et al., 2001; Miller et al., 2005). Therefore, since ACN is best represented by the former relationship, and $H_2O$ by the latter, it is likely that Form I generated from ACN is a more thermodynamically stable form, and Form III generated from slurry experiments in $H_2O$, is metastable. In order to determine if Form III is metastable, we slurried excess Form III in ACN

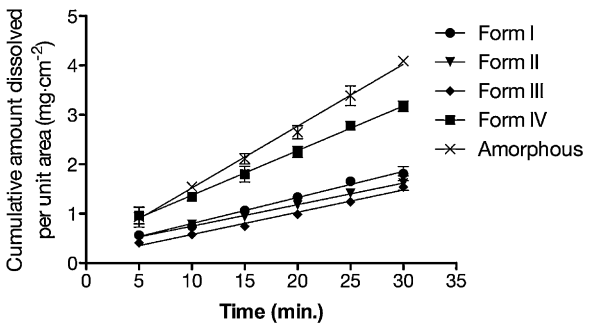


**Fig. 7.** Intrinsic dissolution profiles Form I (●), Form II (▼), Form III (♦), Form IV (■), and amorphous FA (×). $n = 3$; mean ± S.D.

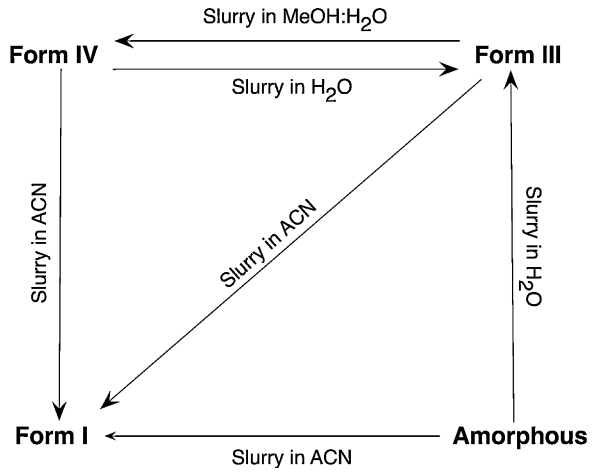


**Fig. 8.** Conversion of FA polymorphic forms by solvent-mediated transformation. *Note*: Form II is generated by recrystallizing any form through the evaporation of DCM at −20 °C, and thus is absent from this figure as it does not occur through solvent-mediated transformation.

for 7 days and found that Form III converts to Form I by 24 h, confirming that Form III is indeed metastable. However, despite the metastable nature of Form III (also the "as received" commercial sample), its stability in $H_2O$ over 28 days suggests that this form is suitable for its commercial use in topical/ocular aqueous suspensions.

Single crystal XRD analysis of Form I yielded a primitive monoclinic lattice system containing two FA molecules, with no evidence of the presence of $H_2O$ or solvent within the lattice. We were unable to generate crystals large enough for single crystal XRD analysis from the other polymorphic forms, and therefore it is unclear how the molecular packing arrangements may differ between the solid forms. Additionally, there is no reference pattern published in peer-reviewed literature, or in any online database (i.e. the Cambridge Structural Database (CSD)) (Allen, 2002). Therefore, this report represents the first published single crystal XRD analysis of FA in the peer-reviewed literature.

DSC and HSM of the bulk FA samples were performed to confirm the presence of the proposed polymorphs. Heating Form IV resulted in several thermal events. The first was a small endotherm with an onset of 120 °C and peak of 128 °C, which was indicative of melting of crystalline drug. When this thermal event was visualized by hot stage microscopy it was confirmed that the crystalline starting material, which displayed a high degree of birefringence, completely melted at 130 °C, resulting in a sample void of any birefringence, thus, confirming that the endotherm at 128 °C was due to melting of crystalline FA. Upon further heating, a large exotherm in the DSC thermogram appeared with a peak at 153 °C, indicative of recrystallization. This recrystallization was confirmed by hot stage microscopy in which crystal growth was observed at 153 °C resulting in the reappearance of birefringence in the sample. Upon further heating, the recrystallized FA finally melted at 175 °C characterized by an endotherm in the DSC thermogram and loss of birefringence when visualized by hot stage microscopy. To investigate the nature of the recrystallized FA at 153 °C, Form IV was evaluated using variable-temperature XRPD. Form IV was heated from to 153 °C at a rate of 5 °C/min, and rapidly cooled to 25 °C using liquid nitrogen. The resulting XRPD pattern of Form IV after heating was different from all other polymorphs (data not shown). However, due to thermal degradation upon heating, as evidenced by sample discoloration and degradation peaks upon HPLC analysis, we were unable to characterize this mixture further.

The DSC thermogram of Forms I, II, and III all displayed single melt endotherms at 190 °C, 178 °C, and 145 °C, respectively. The presence of each thermal event was confirmed by HSM, which displayed the loss of birefringence/melting at the observed endothermic temperatures. Amorphous FA was characterized by a single glass transition at 117 °C. All solid forms displayed an endothermic event at 193 °C, which was due to a thermal degradation event, as it occurred in the temperature range during which rapid mass loss was observed by TGA, and occurred concurrently with the melting of each crystal form (Table 1). Through TGA analysis, we observed that all FA polymorphs (except Form II) gradually lost a small amount of weight over the broad temperature range of 40–150 °C, suggesting the presence of surface adsorbed water. The patent literature claims that FA exists as a hemihydrate (Jensen and Andersen, 2006), which would be characterized as weight loss in a stepwise fashion in a TGA analysis. This was not observed in our experiments, and we found no evidence that the polymorphic forms of FA investigated in this work were hydrates. All samples, regardless of their method of preparation, were characterized by a rapid weight loss at elevated temperatures starting at approximately at 172 °C. This weight loss was attributed to degradation and vaporization of the samples and was further supported by the discolored appearance of the samples upon completion of the run.

To determine if there were any solubility differences between the solid forms of FA, the intrinsic dissolution rates of the solid forms of FA were compared using the rotating disk method using a Wood's apparatus. Given the $pK_a$ of 5.35 for FA, we investigated the IDR at pH 3 and pH 7.4 ($\sim pK_a \pm 2$ pH units) to compare between ionized and unionized drug. However, the concentration of FA in the dissolution media at pH 3 was below the level of detection, and therefore we were unable to quantify the IDR. Thus, for comparison between all forms, the IDR was evaluated at a physiologically relevant pH of 7.4. It was found that Form IV and the amorphous form of FA had greater IDR values (0.092, and 0.125 mg/min/cm$^2$, respectively) than Form I, II or III (IDR of 0.053, 0.043, and 0.045 mg/min/cm$^2$, respectively). It is well known that polymorphism can have a dramatic impact on the solubility of a drug, with more stable polymorphs leading to lower dissolution rates as compared to their metastable counterparts (Grant, 1999). Therefore, the lower solubility of Forms I, II and III suggest much lower lattice energies and an increased stability of these polymorphs compared to Form IV and the amorphous FA. Despite the fact that we were unable to demonstrate any statistical difference between the IDR of Form I, II, or III, even though we would expect the higher melting polymorph (Form I) to have the lowest IDR of all solid forms, our data suggest that there are only minor differences in the lattice energies among Forms I, II, and III. This phenomenon is supported by a literature survey of 55 polymorphic compounds by Pudipeddi et al. who demonstrated that the vast majority of polymorphic forms exhibit limited spread in solubility ratios (solubility of any polymorphic form, normalized to the solubility of the most stable form) or dissolution rates, and is likely due to undetectable differences in the entropy between polymorphs (Pudipeddi and Serajuddin, 2005).

## 5. Conclusions

In this work, we demonstrated that FA undergoes a polymorphic transformation from amorphous or Form IV into Form I, or Form III when slurried in ACN or $H_2O$, respectively. In addition, we have shown that recrystallization of FA, through the evaporation of DCM, yields Form II. Our experiments confirm the existence of Forms I and III, which have been previously reported in the patent literature. Furthermore, we have demonstrated that the commercial form of FA (Form III) is metastable, and converts to Form I in the presence of ACN, but remains stable in aqueous solution. We have also shown the existence of two unreported polymorphic forms of FA (Forms II and IV). Forms I–III had similar IDR values, but were significantly lower than that of Form IV or amorphous. This similarity between IDR values of Forms I–III is likely due to only small lattice energy differences between these forms. Differences in dissolution rates between the polymorphs could conceivably have an impact on the release rate of FA from local delivery devices if the drug was present in the solid-state as Form IV or amorphous FA. However, it is cautioned that formulation of FA as one of theses forms may lead to interconversion to Form III in the presence of an aqueous milieu potentially resulting in a reduction in the release rate of the drug.

## Acknowledgements

The authors would like to thank Dr. Richard Liggins and The Center for Drug Research and Development (CDRD) for the use of their hot stage microscope, and intrinsic dissolution apparatus. The authors would also like to thank Dr. Brian Patrick and Anita Lam for their assistance and use of the Bruker APEX DUO diffractometer. This work would not have been possible without support from the CDRD, and a grant from the Canadian Foundation for Innovation (CFI).

## Appendix A. Supplementary data

Supplementary data associated with this article can be found, in the online version, at doi:10.1016/j.ijpharm.2011.11.005.

## References


Allababidi, S., Shah, J.C., 1998. Kinetics and mechanism of release from glyceryl monostearate-based implants: evaluation of release in a gel simulating in vivo implantation. J. Pharm. Sci. 87, 738–744.

Allen, F.H., 2002. The Cambridge Structural Database: a quarter of a million crystal structures and rising. Acta Crystallogr. B Struct. Sci. 58, 380–388.

Aviv, M., Berdicevsky, I., Zilberman, M., 2007. Gentamicin-loaded bioresorbable films for prevention of bacterial infections associated with orthopedic implants. J. Biomed. Mater. Res. 83A, 10–19.

Ayliffe, G.A., 1997. The progressive intercontinental spread of methicillin-resistant *Staphylococcus aureus*. Clin. Infect. Dis. 24 (Suppl. 1), S74–S79.

Coombs, R.R., 1990. Fusidic acid in staphylococcal bone and joint infection. J. Antimicrob. Chemother. 25 (Suppl. B), 53–60.

Grant, D.J.W., 1999. Theory and origin of polymorphism. Drugs and the Pharmaceutical Sciences, vol. 95, pp. 1–33.

Gu, C.-H, Young, V., Grant, D.J.W., 2001. Polymorph screening: influence of solvents on the rate of solvent-mediated polymorphic transformation. J. Pharm. Sci. 90, 1878–1890.

Howden, B.P., Grayson, M.L., 2006. Dumb and dumber—the potential waste of a useful antistaphylococcal agent: emerging fusidic acid resistance in *Staphylococcus aureus*. Clin. Infect. Dis. 42, 394–400.

Khatib, R., Jose, J., Musta, A., Sharma, M., Fakih, M.G., Johnson, L.B., Riederer, K., Shemes, S., 2011. Relevance of vancomycin-intermediate susceptibility and heteroresistance in methicillin-resistant *Staphylococcus aureus* bacteraemia. J. Antimicrob. Chemother. 66, 1594–1599.

Koort, J.K., Mäkinen, T.J., Suokas, E., Veiranto, M., Jalava, J., Knuuti, J., Törmälä, P., Aro, H.T., 2005. Efficacy of ciprofloxacin-releasing bioabsorbable osteoconductive bone defect filler for treatment of experimental osteomyelitis due to *Staphylococcus aureus*. Antimicrob. Agents Chemother. 49, 1502–1508.

Kurtz, S.M., Lau, E., Schmier, J., Ong, K.L., Zhao, K., Parvizi, J., 2008. Infection burden for hip and knee arthroplasty in the United States. J. Arthroplasty 23, 984–991.

Mader, J.T., Calhoun, J., Cobos, J., 1997. In vitro evaluation of antibiotic diffusion from antibiotic-impregnated biodegradable beads and polymethylmethacrylate beads. Antimicrob. Agents Chemother. 41, 415–418.

Mastrokalos, D.S., Zahos, K.A., Korres, D., Soucacos, P.N., 2006. Arthroscopic debridement and irrigation of periprosthetic total elbow infection. Arthroscopy 22, 1140, e1–3.

Maviglia, R., Nestorini, R., Pennisi, M., 2009. Role of old antibiotics in multidrug resistant bacterial infections. Curr. Drug Targets 10, 895–905.

Mendel, V., Simanowski, H.-J., Scholz, H.C., Heymann, H., 2005. Therapy with gentamicin-PMMA beads, gentamicin-collagen sponge, and cefazolin for experimental osteomyelitis due to Staphylococcus aureus in rats. Arch. Orthop. Trauma Surg. 125, 363–368.

Miller, J., Collman, B., Greene, L., Grant, D., Blackburn, A., 2005. Identifying the stable polymorph early in the drug discovery-development process. Pharm. Dev. Technol. 10, 291–297.

O'Neil, M.J., 2006. In: O'Neil (Ed.), The Merck Index: An Encyclopedia of Chemicals, Drugs, and Biologicals. , 14th ed. Merck.

Pudipeddi, M., Serajuddin, A.T.M., 2005. Trends in solubility of polymorphs. J. Pharm. Sci. 94, 929–939.

Reeves, D., 1987. The pharmacokinetics of fusidic acid. J. Antimicrob. Chemother. 20, 467–476.

Jensen, J., Andersen, N.R., 2006. Preparation of a Crystalline Antibiotic Substance. US Patent Office (12084231).

Schierholz, J.M., Steinhauser, H., Rump, A.F., Berkels, R., Pulverer, G., 1997. Controlled release of antibiotics from biomedical polyurethanes: morphological and structural features. Biomaterials 18, 839–844.

Schmitz, F.J., Sadurski, R., Kray, A., Boos, M., Geisel, R., Köhrer, K., Verhoef, J., Fluit, A.C., 2000. Prevalence of macrolide-resistance genes in *Staphylococcus aureus* and *Enterococcus faecium* isolates from 24 European university hospitals. J. Antimicrob. Chemother. 45, 891–894.

Sisirak, M., Zvizdic, A., Hukic, M., 2010. Methicillin-resistant *Staphylococcus aureus* (MRSA) as a cause of nosocomial wound infections. Bosn J. Basic Med. Sci. 10, 32–37.

Spelman, D., 1999. Fusidic acid in skin and soft tissue infections. Int. J. Antimicrob. Agents. 12 (Suppl. 2), S59–S66.

Toh, S.-M., Xiong, L., Arias, C.A., Villegas, M.V., Lolans, K., Quinn, J., Mankin, A.S., 2007. Acquisition of a natural resistance gene renders a clinical strain of methicillin-resistant *Staphylococcus aureus* resistant to the synthetic antibiotic linezolid. Mol. Microbiol. 64, 1506–1514.

Trampuz, A., Zimmerli, W., 2006. Antimicrobial agents in orthopaedic surgery: prophylaxis and treatment. Drugs 66, 1089–1105.

Winkler, H., Stoiber, A., Kaudela, K., Winter, F., Menschik, F., 2008. One stage uncemented revision of infected total hip replacement using cancellous allograft bone impregnated with antibiotics. J. Bone Joint Surg. Br. 90, 1580–1584.

Yang, C., Plackett, D., Needham, D., Burt, H.M., 2009. PLGA and PHBV microsphere formulations and solid-state characterization: possible implications for local delivery of fusidic acid for the treatment and prevention of orthopaedic infections. Pharm. Res. 26, 1644–1656.

Yang, S.J., Nast, C.C., Mishra, N.N., Yeaman, M.R., Fey, P.D., Bayer, A.S., 2010. Cell wall thickening is not a universal accompaniment of the daptomycin nonsusceptibility phenotype in *Staphylococcus aureus*: evidence for multiple resistance mechanisms. Antimicrob. Agents Chemother. 54, 3079–3085.

Zimmerli, W., Ochsner, P., 2003. Management of infection associated with prosthetic joints. Infection 31, 99–108.